https://doi.org/10.5194/hess-2021-364
Preprint. Discussion started: 7 September 2021

Hydrology and Earth System Sciences Discussions
Open Access

Contrasting lacustrine groundwater discharge and associated nutrient loads in different geological conditions

Xiaoliang Sun[1], Yao Du[1,2]*, Yamin Deng[1,2], Hongchen Fan[1,2], Teng Ma[1,2]

[a] *Hubei Key Laboratory of Yangtze Catchment Environmental Aquatic Science, School of Environmental Studies, China University of Geosciences, Wuhan 430078, China*

[b] *State Key Laboratory of Biogeology and Environmental Geology, China University of Geosciences, Wuhan 430078, China*

Abstract. The spatial patterns of lacustrine groundwater discharge (LGD) and associated nutrients input is crucial for effective management and protection of lakes. Multiple factors have been found to influence the spatial differences in LGD rates and associated nutrients loads, but the influence of geological conditions on the differences have not been well understood. In this study, we quantified LGD rates and associated nutrients loads in two sides with contrasting geological conditions of East Dongting Lake (EDL) within central Yangtze catchment and discuss the influence of geology on the spatial differences, through ^{222}Rn mass-balance model, water chemistry coupled with existing geological data. The results showed that LGD rates were 38.66 ± 21.07 mm d^{-1} in the east EDL which is characterized by hilly geomorphy, deep/fast/narrow flowing, coarse-grained lakebed and large hydraulic gradients (0.004 - 0.006). Surprisingly, LGD rates were higher (92.82 ± 51.98 mm d^{-1}) in the west EDL which is characterized by alluvial-lacustrine plain geomorphology, shallow/sluggish flowing, clayey or silty lakebed and low hydraulic gradients (0.0002 - 0.0015). The remaining factor determining the higher LGD rates in the west EDL is the permeability of the porous aquifer connected with the lake, which could be enlarged by some preferential pathways including large-scale buried paleo-channel and small-scale plant roots. The groundwater around the east EDL existed in a less confined environment, and frequent flushing led to low concentrations of nutrients. On the contrast, rapid burial of sediments and deposition of paleo-lake sediments since Last Deglaciation formed an

* Correspondence to: Yao Du, School of Environmental Studies, China University of Geosciences, Jincheng Road 68, Wuhan 430078, China.

E-mail address: yaodu@cug.edu.cn (Yao Du)

https://doi.org/10.5194/hess-2021-364
Preprint. Discussion started: 7 September 2021

Hydrology and Earth System Sciences Discussions
Open Access

organic-rich and reducing environment, which facilitated the enrichment of geogenic nutrients. As a result, the loads of LGD-derived nutrients in the west generally exceeded that in the east by one order of magnitude. In practice, future water resource management and ecological protection of Dongting Lake should focus on groundwater discharge in west EDL. This study highlights an important role of geological conditions in determining contrasting LGD rates and associated nutrients loads in large freshwater lakes.

1 Introduction

Recent studies have shown that groundwater is an important component of lake water (Kong et al., 2019; Kidmose et al., 2013; Stets et al., 2010; Schmidt et al., 2009; Roy and Hayashi., 2008) and lake chemistry (Kazmierczak et al., 2020; Kong et al., 2019; Luo et al., 2018; Burnett et al., 2017; Meinikmann et al., 2015) globally. Lacustrine groundwater discharge (LGD) has received increased interest among researchers due to its impacts to lake water. LGD and LGD-derived nutrients can result in a deterioration of lake water quality and phytoplankton blooms (Holman et al., 2008; Krest et al., 2000), consequently negatively effecting the aquatic ecosystem of a lake. Therefore, there is an urgent need for the quantification of the contributions of LGD to lake water and nutrients balances, thereby providing a new perspective on lake water resources management and aquatic ecosystem protection.

LGD and associated nutrients input are often characterized by large spatial variability due to the heterogeneity of geomorphy, surface hydrology, lakebed sediment lithology, hydrogeology, nutrient concentration levels of groundwater around lakes, etc (Wallace et al., 2020; Tecklenburg and Blume, 2017; Hare et al., 2017; Rosenberry et al., 2015; Meinikmann et al., 2015, 2013; Blume et al., 2013; Schneider et al., 2005). For example, Schmidt et al. (2010) found that LGD rates were related to the drainage area/lake area ratio which promotes greater surface connectivity. Meinikmann et al. (2015) observed that both the intensity of the contamination and its proximity to the lake inhibit nutrient retention within vadose zone and aquifer and allow significant phosphorus loads to be discharged into the lake. Tecklenburg and Blume (2017) found that large-scale LGD patterns were correlated with topography and groundwater flow field, whereas small-scale patterns correlated with grain size distributions of the lake sediment. However, the influence of geological conditions on spatial differences in LGD and associated nutrients input have not been well understood. Moreover, the geological factor could be internally inter-played with hydrogeology, groundwater quality and even

https://doi.org/10.5194/hess-2021-364
Preprint. Discussion started: 7 September 2021

Hydrology and Earth System Sciences
Open Access
EGU
Discussions

super-surface factors mentioned above, which may collaboratively lead to spatial variability in LGD and associated nutrients input. The advancing of related understanding may require a comprehensive analysis from the perspective of geology.

Dongting Lake had previously been recognized as the largest fresh lake in China by surface area. However, the lake has gradually contracted due to natural sedimentation and land reclamation in recent decades, and is currently recognized as the second largest fresh lake in China (Yu et al., 2020; Yi, 2017). Dongting Lake also hosts one of the most ecologically important wetlands in the Yangtze Catchment. This wetland has been referred to as the "kidney of Yangtze River" in recognition of its important function in water purification, and also has vital roles in water conservation, climate regulation, and biodiversity conservation (Hu et al., 2020; Zheng et al., 2016; Pan et al., 2013). Groundwater is abundant around Dongting Lake (Huang et al., 2019), and the quality of this groundwater is poor due to the influence of anthropogenic activities and natural processes (Huang et al., 2021; Long et al., 2021). However, the role of groundwater in the balance of water and chemicals in Dongting Lake remains poorly understood. Although some studies have identified the strong exchange between groundwater and lake water (Zhan et al., 2014) and considerable contribution of groundwater to overall water and nutrient balances of Dongting Lake (Sun et al., 2020), the spatial contrast of LGD and associated nutrient loads has not yet studied.

East Dongting Lake (EDL) is a relatively independent part of Dongting Lake and is also recognized as a wetland of international importance by the Ramsar Convention (Zou et al., 2019; Liu et al., 2019). The EDL plays an important function in regulating the flood runoff of the Yangtze River and also hosts rare birds and the Yangtze River dolphin (Zou et al., 2019; Xie, 2017; Xiong et al., 2016). The current water resource and ecological statuses of the EDL are poor relative to historical conditions due to a deterioration in water quality, ecological degradation, and a decline in species diversity as a result of lake shrinkage and wetland degradation (Huang et al., 2018; Wang et al., 2015; Wang et al., 2015; Hu et al., 2015). The ecological sensitivity and important ecological role of the EDL emphasize the need for an evaluation of LGD and associated nutrients input. The west side and east side of EDL are characterized by contrasting geological conditions, with which significant differences can be observed in geomorphy, surface hydrology, lakebed sediment lithology, hydrogeology, etc (details in site description). The differences in these factors between the west and east EDL are expected to result in spatial differences in LGD and associated nutrients input.

https://doi.org/10.5194/hess-2021-364
Preprint. Discussion started: 7 September 2021

Although various methods of quantifying LGD exist (Tecklenburg and Blume; 2017; Dimova et al., 2015; Lewandowski et al., 2013; Stets et al., 2010), radioactive ^{222}Rn tracing has been widely and effectively used in recent years (Wallace et al., 2021, 2020; Dabrowski et al., 2020; Hare et al., 2017; Petermann et al., 2018; Liao et al., 2018; Luo et al., 2018, 2016, 2014; Burnett et al., 2017; Dimova et al., 2015, 2013; Gilfedder et al., 2015; Peterson et al., 2010; Schmidt et al., 2010, 2009). ^{222}Rn is a subset of ^{226}Ra and is widely present in inland rocks and water bodies. Uranium-bearing minerals in sediments continuously release ^{222}Rn during decay, resulting in the ^{222}Rn concentration in groundwater typically being much higher than that in surface water. ^{222}Rn is an inert gas that is chemically conservative. Since ^{222}Rn in lake water mainly originates from groundwater, the spatial distribution of ^{222}Rn in lake water can to a certain extent act as an indicator of the spatial distribution of LGD if it is assumed that the ^{222}Rn concentration in groundwater is relatively uniform (Cheng et al., 2020; Wallace et al., 2020; Burnett et al., 2017). A mass-balance model can be established based on the ^{222}Rn source and sink terms, thereby allowing LGD to be calculated as the single unknown term controlling ^{222}Rn in lake water. Although ^{222}Rn mass balance model has been widely used, it was rarely applied in large freshwater lake system with complex geological conditions.

The present study aims to identify and quantify the spatial differences in LGD and associated nutrients input in the EDL, and discuss the influence of multiple factors on the spatial differences from a comprehensive perspective of geology, through ^{222}Rn mass-balance model, water chemistry coupled with existing geological data. The present study provides new understanding of the spatial differences in LGD and associated nutrients input to the EDL resulting from variations in geological conditions, thus serving as a reference for ecological protection of EDL. The knowledge from this study could be applicable for other large freshwater lakes under humid climate worldwide.

2 Materials and methods

2.1 Site description

The EDL is located in the middle reaches of the Yangtze River (28° 59' N–29° 38' N, 112° 43' E–113° 15' E) and on the northeast side of Dongting Lake (Fig. 1b). The EDL has an area of 1300 km^2 during the flood season (Huang et al., 2018), and falls within a subtropical monsoonal climate zone, with an annual average temperature and annual average precipitation of 16.4 °C–17.0 °C and 1300–1700 mm, respectively, with 70% of annual precipitation concentrated during April–August. The southern part of the EDL receives water from West Dongting Lake and South Dongting Lake fed by four larger rivers (Xiangjiang, Zishui, Yuanjiang, and Lishui rivers) originate from the southern and western mountainous areas of the Dongting Lake Basin and three smaller rivers (Songzi, Hudu, and Ouchi rivers) originate from the Yangtze River (Li and Yang, 2016; Sun et al., 2018). All the water from the Dongting Lake empties into the Yangtze River at Chenglingji in the EDL (Fig. 1b).

The EDL can be divided into two parts, namely the eastern and western parts of the EDL (EEDL and WEDL, respectively), with Junshan Island acting as a boundary (Fig. 1c). The EEDL and WEDL show obvious differences in geomorphology, surface hydrology, lakebed sediment lithology, hydrogeology, etc. Water flows from upstream into the EEDL and all water leaves the lake at Chenglingji in the EEDL (Fig. 1c). The EEDL is characterized as deep and fast flowing, with which pebble, gravel, and fine-coarse sand are deposited in the lakebed. The EEDL is surrounded by hilly area in which the main aquifer type is fissured aquifer composed of intrusive or metamorphic rocks. The porous aquifer is only found on the shore of the EEDL in which there are a few river terraces. On the contrast, the WEDL receives little surface runoff during the dry season. The WEDL is shallow and has a quite slow flow rate, with which clay, silty clay, and fine-coarse sand are deposited in the lakebed. The WEDL is surrounded by alluvial-lacustrine plain in which Quaternary porous aquifers are widely distributed. These aquifers are mainly composed of 2-layer or 3-layer structures, as well as single-layer structures in some areas (Fig. 1d). The first aquifer is a phreatic aquifer with a thickness of less than 20 m and is mainly composed of clay, silty clay, and clayey silt, interlaced locally with silt or fine sand. The second aquifer is a confined aquifer dominated by fine-medium sand, locally interlaced with gravel, and has a thickness of 50–150 m (Sun et al., 2020; Wang, 2015). The third aquifer is also a confined aquifer and is mainly composed of gravel and coarse sand, with a thickness of 50–100 m (HGSI, 2016).

The depth of the EDL is generally less than 20 m. Around the EEDL, the fissured aquifer is directly connected to the lake. Around the WEDL, the phreatic aquifer is exposed at the edge of the lake and is connected with the shallow area of the lake. The porous confined aquifer is more likely to be connected with the deeper area of the lake. There is a seasonally inundated area between the EEDL and WEDL, which becomes a mud flat during the dry season. The regional groundwater flow field shows that groundwater below this intermediate area flows parallelly to the shore of both EEDL and WEDL (Fig. S1), so lateral groundwater flow to the EEDL and WEDL can be ignored in this study.

https://doi.org/10.5194/hess-2021-364
Preprint. Discussion started: 7 September 2021

Hydrology and Earth System Sciences
Discussions
Open Access

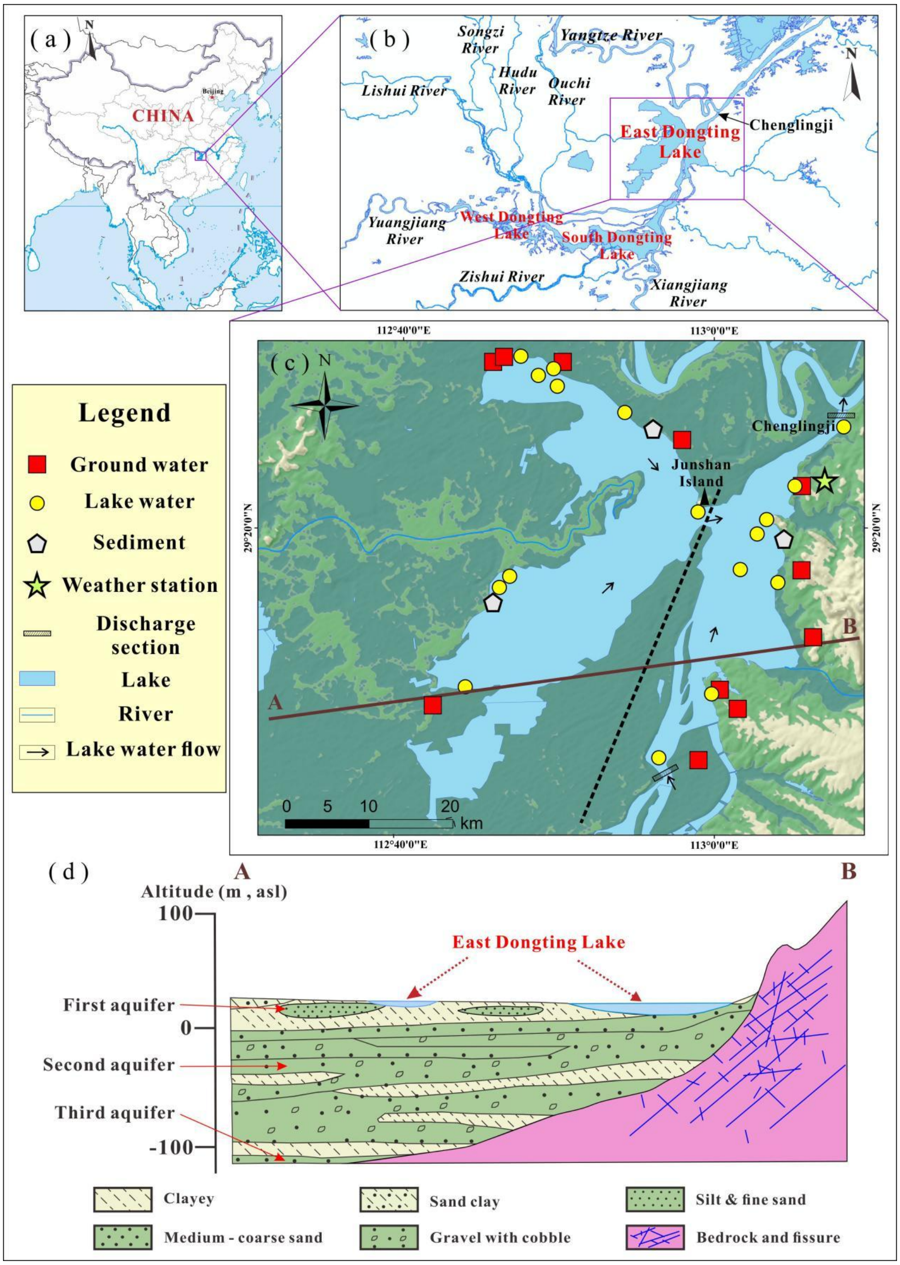

Figure 1. (a): The location of Dongting Lake in China. **(b)**: the location of East Dongting Lake (EDL). The topographical information is from Geospatial data cloud (http://www.gscloud.cn/sources/index?pid=302). **(c)**: the distributions of sampling sites in which the dotted black line represents the boundary between the West EDL (WEDL) and East EDL (EEDL). **(d)**: a typical section shown as a solid brown line (A–B) **(c)**.

2.2 Field work and laboratory measurements

https://doi.org/10.5194/hess-2021-364
Preprint. Discussion started: 7 September 2021

Field sampling was conducted from January 10, 2019 to January 20, 2019 and from January 10, 2020 to January 14, 2020. A total of 32 samples were collected from within and around the EDL, including 17 lake samples, 12 groundwater samples, and 3 sediment samples (Fig. 1c). Lake water samples were collected at a depth of 0.5 m and as far as possible from the lake shore using surface water collection equipment. Two methods were used to collect groundwater. Under the first method, groundwater samples were collected from local wells at a depth of 5–30 m and within 3 km from the lake shore. Under the second method, a push point and a peristaltic pump are used to collect pore water samples from a depth of 1 m in the lake shore. In the field, all water samples were immediately filtered through a 0.45 μm membrane filter. Samples for analysis of cations were collected in 30 mL polyethylene bottles and acidified with concentrated HNO_3 to a pH < 2. The water samples for ^{222}Rn analysis were collected in 250-mL or 40-mL glass bottles. All collected water samples contained no captured air. Sediment samples were collected from the lakebed on the western, northern, and eastern shores of the EDL for the measurement of the concentration of ^{222}Rn in the pore water of sediments. In addition, lake water and groundwater levels were measured by a differential global positioning system (GPS) to identify the exchange relationship between groundwater and lake water.

A multi-parameter handheld meter (HACH HQ40D, USA) was used to measure the field parameters of water samples, including pH, water temperature, electrical conductivity (EC), dissolved oxygen (DO) and redox potential (Eh). A portable spectrophotometer (Hach 2800, USA) was used to measure NH_4-N and Fe^{2+} in the field. Inductively coupled plasma optical emission spectrometry (ICP-AES) (iCAP 6000 series, Thermo Fisher Scientific, USA, detection limits: 0.001 mg/L) was used to analyze the concentration of cations. A Water Isotope Analyzer (LGR, IWA-45EP) were used to determine the δ^2H-H_2O and $\delta^{18}O$-H_2O values with the precision of 0.5‰ for δ^2H and 0.2‰ for $\delta^{18}O$. ^{222}Rn concentrations were measured using a RAD7 H_2O instrument in the field. Since the half-life of ^{222}Rn is very short, the sampling time was recorded, and the true ^{222}Rn concentration was corrected as:

$$A_t = A \times e^{\lambda t}, \quad (1)$$

In Eq. (1), A_t is the ^{222}Rn concentration at sampling time (Bq m^{-3}), A is the ^{222}Rn concentration at measurement time (Bq m^{-3}), λ is decay coefficient of ^{222}Rn, and t is the time interval from sampling to measurement.

2.3 ^{222}Rn mass-balance model

https://doi.org/10.5194/hess-2021-364
Preprint. Discussion started: 7 September 2021

The ^{222}Rn mass-balance model was used to quantify LGD fluxes based on the balance relationship between source and sink terms (Fig. 2). The mass-balance model can be expressed as (Dabrowski et al., 2020; Sun et al., 2020; Liao et al., 2018; Luo et al., 2016; Schmidtet al., 2009; Kluge et al., 2007):

$$\frac{\partial I^{222}Rn}{\partial t} = F_g + F_d + I^{226}Ra \times \lambda^{222}Rn + F_s - F_a - I^{222}Rn \times \lambda^{222}Rn - F_o, \quad (2)$$

In Eq. (2), F_g, F_d, F_s, F_a, and F_o are ^{222}Rn fluxes (Bq m^{-2} d^{-1}) for groundwater discharge, sediment diffusion, river inflow, atmospheric loss, and lake outflow, respectively, $I^{226}Ra$ and $I^{222}Rn$ are ^{226}Ra and ^{222}Rn pools in lake water (Bq m^{-2}) that are equal to the concentrations of ^{226}Ra and ^{222}Rn in the lake water multiplied by the lake water depth, respectively, and $\lambda^{222}Rn$ is the decay constant of ^{222}Rn with a value of 0.186 d^{-1}. The left-hand side of Eq. (2) represents the change in ^{222}Rn in the lake water over time, with a value equal to 0 due to the insignificant change.

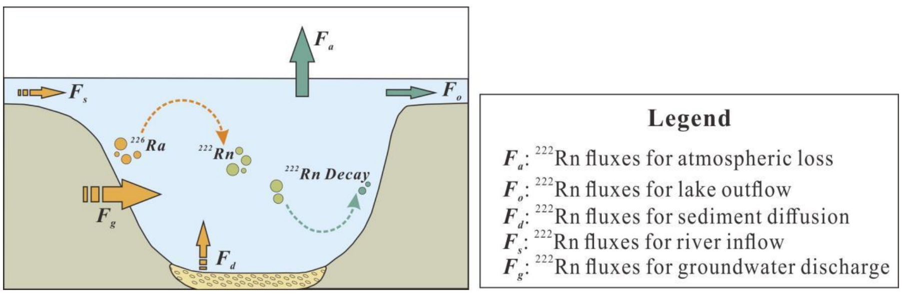

Figure 2. A conceptual diagram of the ^{222}Rn mass-balance model. The orange and green arrows represent the sources and sinks of the ^{222}Rn mass-balance model, respectively.

The groundwater discharge rate equation was used to estimate groundwater discharge into the EDL (Luo et al., 2016; Liao et al., 2018):

$$V = \frac{F_g}{C_g}, \quad (3)$$

In Eq. (3), V is the groundwater discharge rate (m d^{-1}), F_g (Bq m^{-2} d^{-1}) is the groundwater ^{222}Rn flux, and C_g (Bq m^{-3}) is the ^{222}Rn concentration in groundwater.

The loss of ^{222}Rn to the atmosphere was estimated based on an empirical equation that takes into account wind speed and air temperature (Luo et al., 2016; Schubert et al., 2014; Dimova and Burnett, 2011; Macintyre et al., 1995):

$$F_a = k(c_w - \partial c_a), \quad (4)$$

$$\partial = 0.105 + 0.405 \times e^{-0.05027 \times T_a}, \quad (5)$$

https://doi.org/10.5194/hess-2021-364
Preprint. Discussion started: 7 September 2021

$$K = 0.45\,\mu^{1.6} \times \left(\frac{S_C}{600}\right)^{-b}, \tag{6}$$

$$S_C = 3417.6 \times e^{-0.0634 \times T_a}, \tag{7}$$

In Eq. (4–7), K is the gas transfer coefficient (m d^{-1}), C_w and C_a are the concentrations of ^{222}Rn in lake water and air, respectively (Bq m^{-3}), α is the gas distribution coefficient, b equals to 0.5 and 0.667 when wind speed is ≥ 3.6 m s^{-1} and < 3.6 m s^{-1}, respectively, T_a is air temperature (°C); μ is the wind speed at 10 m above the lake surface.

The ^{222}Rn flux from the lakebed sediment to the lake is calculated as (Luo et al., 2016):

$$F_d = \left(\lambda^{222}Rn \times D_s\right)^{0.5}\left(C_p - C_w\right), \tag{8}$$

In Eq. (8), λ^{222}Rn is the decay constant of ^{222}Rn and has a value of 0.186 $^{-1}$, C_p (Bq m^{-3}) is the average radon concentration of pore water in sediments, C_w (Bq m^{-3}) is the ^{222}Rn concentration of overlying water. The ^{222}Rn concentration in sediment pore water was obtained by equilibrium incubation experiment (Corbett et al., 1997). The D_S (m d^{-1}) is the radon molecular diffusion coefficient in wet bulk sediment depending on the molecular diffusion coefficient (D_m) in lake water and the porosity (n) of the sediment (Boudreau, 1996). D_S and D_m are expressed as:

$$D_S = \frac{D_m}{\left[1 - \ln(n^2)\right]^2}, \tag{9}$$

$$-\log D_m = \left(\frac{980}{T}\right) + 1.59, \tag{10}$$

An equilibrium incubation experiment with lakebed sediments was carried out to obtain the ^{222}Rn concentration in sediment pore water (Corbett et al., 1998). 150 g of sediment and 500 mL of in-situ lake water were placed in an Erlenmeyer flask and sealed. The lakebed sediment and overlying lake water were incubated in a shaker for 30 days until the ^{222}Rn concentration in sediment pore water reached equilibrium. The balanced lake water was transferred to 250 mL glass bottles by overflow method and then measured with RAD7 and RAD H_2O. The concentration of ^{222}Rn in sediment pore water can be calculated as:

$$C_p = \frac{C_s \times \rho_w}{n}, \tag{11}$$

$$C_s = \frac{A_0 \times V_0}{M_s}, \tag{12}$$

Hydrology and Earth System Sciences
Open Access
Discussions

In Eq. (11–12), C_s is the ^{222}Rn concentration in unit volume wet sediment (Bq kg^{-1}), ρ_w is wet density of sediment (kg m^{-3}), n is the porosity of sediment, A_0 is the ^{222}Rn concentration in overlying water (Bq m^{-3}) at equilibrium, V_0 and M_s are the lake water volume (m^3) and sediment mass (kg) used in the equilibrium experiment, respectively.

3 Results

3.1 Field parameters

Table S1 shows the parameters of different water bodies in the EDL that were measured in the field. The groundwater levels around the EDL ranged from 23.2 to 41.9 m, whereas the lake water levels varied from 21.2 to 22.4 m. The higher groundwater levels compared to lake levels suggested groundwater discharge to the lake. The average temperature, pH, redox potential (Eh), electrical conductivity (EC), and dissolved oxygen (DO) of lake water samples were 6.81 ± 1.76 °C, 7.91 ± 0.26, 146.7 ± 61.6 mV, 395.9 ± 139.1 μS cm^{-1}, and 11.33 ± 0.64 mg L^{-1}, respectively. Groundwater had a higher temperature (15.74 ± 3.30 °C) and EC (518 ± 208 μS cm^{-1}) but lower pH (7.23 ± 0.63), Eh (16.94 ± 139.74 mV), and DO (3.5 ± 0.7 mg L^{-1}) as compared with lake water.

Groundwater levels and lake levels varied spatially, ranging from 15.6 to 20.4 m, far exceeding the level of the WEDL (0.8 to 2.8 m). The average temperature, pH, Eh, EC, and DO of lake water samples in the EEDL were 7.89 ± 1.62 °C, 7.80 ± 0.32, 148.83 ± 80.82 mV, 291.75 ± 18.25 μS cm^{-1}, and 11.11 ± 0.16 mg L^{-1}, respectively; those of groundwater samples in the EEDL were 15.88 ± 0.41 °C, 6.82 ± 0.50, 98.45 ± 167.60 mV, 425.50 ± 269.31 μS cm^{-1}, and 4.42 ± 1.84 mg L^{-1}, respectively; those of lake water samples in the WEDL were 5.86 ± 1.32 °C, 8.00 ± 0.15, 144.77 ± 43.04 mV, 488.56 ± 133.86 mg L^{-1}, and 11.53 ± 0.84 mg L^{-1}, respectively; those of groundwater samples of the WEDL were 15.60 ± 1.24 °C, 7.51 ± 0.57, −37.40 ± 97.12 mV, 579.17 ± 349.95 μS cm^{-1}, and 4.02 ± 3.00 mg L^{-1}, respectively（Table S1）. The average EC of lake water in the EEDL exceeded that in the WEDL. The difference in EC of lake water between the EEDL and WEDL can be attributed to different sources of water. The difference in Eh of surrounding groundwater between the EEDL and WEDL was significant and groundwater around the WEDL existed in a more reducing environment.

3.2 Stable isotopic characteristics

Table S1 shows the results of $\delta^{18}O$ analysis of lake water and groundwater. The mean values of

$\delta^{18}O$ in the lake water and groundwater were −5.27‰ and −6.30‰, respectively. Figure 3 shows the relationship between $\delta^{18}O$ and δD values for all water samples. All the lake water samples and groundwater samples were positioned near the local meteoric water line ($\delta D = 8.4 \times \delta^{18}O + 17.3$) (Wu et al., 2012), indicating that both lake water and groundwater around the EDL originated from precipitation. In general, the $\delta^{18}O$ of lake water exceeded that in groundwater, indicating a stronger evaporation in lake water (Zhao et al., 2018; Birks et al., 2017). However, groundwater had a relatively higher $\delta^{18}O$ in the hilly area of the EEDL, indicating that the groundwater had experienced strong evaporation or strong recharge by precipitation (the $\delta^{18}O$ value of winter precipitation in the Dongting Lake area was −5.61‰ to −2.92‰) (Huang, 2013). This indicated that the groundwater in the EEDL existed in a less confined environment. In contrast, groundwater in the WEDL had a lower $\delta^{18}O$ value, suggesting less influence from evaporation.

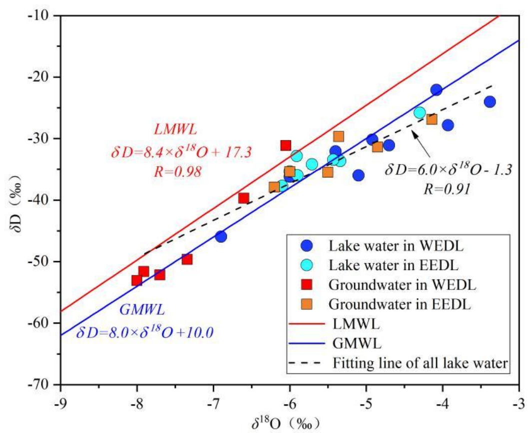

Figure 3. The relationship between δD and $\delta^{18}O$ in lake water and groundwater of East Dongting Lake (EDL), China. The lake water sampling points are represented by solid circles, among which the dark blue and light blue circles represent West EDL (WEDL) and East EDL (EEDL), respectively. Each groundwater sampling point is represented by a solid square, with deep red and light red squares representing the WEDL and EEDL, respectively. The local meteoric water line (LMWL) represents the precipitation line in Changsha, Hunan Province, China. Abbreviations: GMWL – global meteoric water line (Wu et al., 2012).

3.3 Distribution of ^{222}Rn concentrations

Figure 4 shows the spatial distribution of ^{222}Rn concentrations in lake water and groundwater. The average ^{222}Rn concentrations of lake water and groundwater were 245.10 ± 180.61 Bq m^{-3} and 6636.42 ± 5432.80 Bq m^{-3}, respectively. ^{222}Rn concentration showed high spatial heterogeneity in both lake water and groundwater. The ^{222}Rn concentration in the EEDL ranged from 99.44 to 288.57 Bq m^{-3}, with

https://doi.org/10.5194/hess-2021-364
Preprint. Discussion started: 7 September 2021

an average of 154.80 ± 60.33 Bq m^{-3}, whereas that in groundwater of the EEDL ranged from 2493.26 to 19821.17 Bq m^{-3}, with an average of 9464.64 ± 6049.75 Bq m^{-3}. The ^{222}Rn concentration in the WEDL ranged from 109.80 to 700.72 Bq m^{-3}, with an average of 325.36 ± 215.99 Bq m^{-3}, whereas that of groundwater in the WEDL ranged from 2037.83 to 5191.34 Bq m^{-3}, with an average of 3242.54 ± 1281.61 Bq m^{-3}. The difference in ^{222}Rn concentration between groundwater and lake water in the EEDL exceeded that in the WEDL. Most of the ^{222}Rn in lake water originates from groundwater (Yang et al., 2020; Burnett et al., 2017). Therefore, similarity in ^{222}Rn concentration between lake water and groundwater indicates that lake water is strongly affected by groundwater. Hence, it can be assumed that the WEDL was more strongly affected by groundwater discharge as compared to the EEDL.

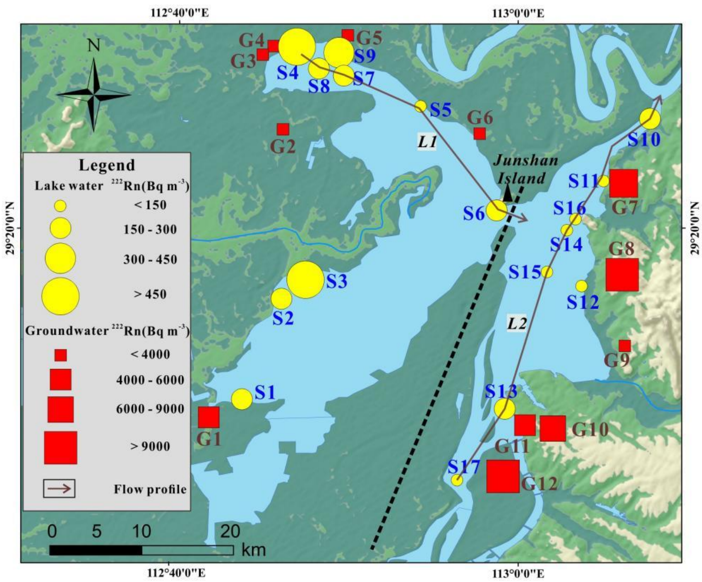

Figure 4. The distribution of ^{222}Rn concentration in lake water and groundwater of East Dongting Lake (EDL), China. The lake water sampling points are represented by yellow solid circles where the circle size represents ^{222}Rn concentration. The groundwater sampling points are represented by red solid squares where square size represents ^{222}Rn concentration. The dotted black line represents the boundary between the West EDL (WEDL) and East EDL (EEDL). The solid lines with dark gray arrows show the flow profile, L1 in the WEDL and L2 in the EEDL, and the arrows represent the flow direction. The topographical information is from Geospatial data cloud (http://www.gscloud.cn/sources/index?pid=302).

4 Discussion

4.1 Identifying occurrence of LGD

Two flow profiles (L1 and L2) were selected in the WEDL and EEDL (Fig. 4). The concentration

https://doi.org/10.5194/hess-2021-364
Preprint. Discussion started: 7 September 2021

Hydrology and Earth System Sciences Discussions
Open Access

of ^{222}Rn is expected to decrease with increasing lake flow due to its short half-life and atmospheric loss. However, the ^{222}Rn concentrations in the S8–S7 and S5–S6 sections of the L1 flow profile in the west and the S17–S13, S15–S14, S14–S11, and S11–S10 sections of the L2 flow profile in the east increased with increasing flow, indicating that ^{222}Rn likely originated from groundwater discharge in these sections (Qin et al., 2020; Yang et al., 2020). This assertion is supported by the δ^{18}O signatures along these two flow profiles. The δ^{18}O value of the lake water is expected to increase along the flow profile as the lake water evaporates in the absence of the lake inflow. A decrease in the δ^{18}O value of the lake water along the flow profile may indicate the presence of an end member with a lower δ^{18}O value. It is likely that groundwater is the external source of water when there is no surface water input perpendicular to the flow profile (Liao et al., 2020; Qin et al., 2020; Liao et al., 2018). The δ^{18}O value of groundwater was lower than that of lake water in the L1 profile. Therefore, LGD occurred along the area showing a lower δ^{18}O value of flowing lake water. As shown in Fig. 5a, the area of LGD as indicated by δ^{18}O on the L1 profile was consistent with the area of LGD indicated by ^{222}Rn. The δ^{18}O of groundwater in the L2 profile exceeded that of lake water in most areas. Therefore, areas in which lake δ^{18}O was elevated (Fig. 5b) may have been affected both evaporation and groundwater discharge.

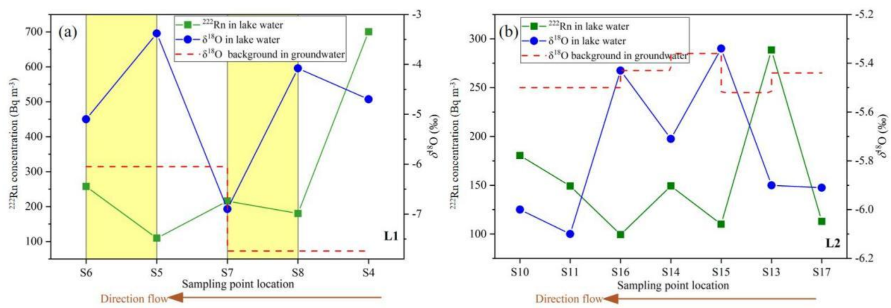

Figure 5. Variations in ^{222}Rn concentrations and δ^{18}O values along the L1 and L2 flow profiles in the Western part of East Dongting Lake (WEDL) **(a)** and East EDL (EEDL) **(b)**, China. The horizontal axis from right to left represents lake water sampling points of the L1 and L2 profiles along the flow direction.

The EC of groundwater generally exceeded that of lake water. Therefore, the EC of lake water will be higher in areas in which LGD is more intensive. A fairly strong correlation between ^{222}Rn and EC in the WEDL was identified ($R^2 = 0.59$, $P < 0.001$) (Fig. 6a), whereas that in the EEDL was insignificant ($R^2 = 0.18$, $P > 0.05$) (Fig. 6b). This result further confirms the greater influence of LGD on lake water in the WEDL as compared to that in the EEDL.

https://doi.org/10.5194/hess-2021-364
Preprint. Discussion started: 7 September 2021

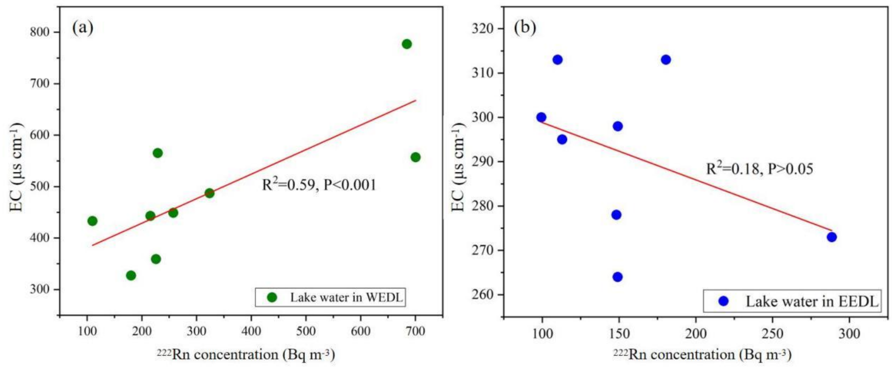

Figure 6. The relationship between ^{222}Rn and electrical conductivity (EC) in lake water of the Western part of East Dongting Lake (WDEL) **(a)** and East EDL (EEDL) **(b)**, China. The horizontal and vertical axes represent ^{222}Rn concentration and conductivity, respectively. The WEDL and EEDL are represented by the green and blue dots, respectively.

4.2 Quantifying LGD fluxes

4.2.1 Quantifying LGD in the WEDL

There is little inflow into the WEDL and little water outflow from the WEDL during the dry season. Therefore, the input and output of ^{222}Rn from the WEDL can be ignored during the dry season.

Wind speed and temperature monitoring data for the study period were obtained from the Yueyang Station of the China Meteorological Network (http://www.cma.gov.cn/). These data showed a daily average wind speed of 2.54 m s^{-1} and an air temperature of 5.33 °C. The atmospheric ^{222}Rn concentration was determined to be 8.11 Bq m^{-3}. Equation (4) was used to calculate an atmospheric ^{222}Rn loss flux of 261.84 ± 138.41 Bq m^{-2} d^{-1}. The average water depth of the WEDL during the study period was 0.8 m whereas the ^{222}Rn decay flux was determined to be 48.56 ± 32.14 Bq m^{-2} d^{-1}.

Typically, ^{222}Rn originating from the decay of dissolved ^{226}Ra can be ignored within the ^{222}Rn mass-balance model (Yi et al., 2018). This assertion was verified by a simple experiment in which two lake water samples were degassing and then sealed (Corbett et al., 1997). ^{222}Rn was not detected in either of the two lake water samples after 28 days, indicating that ^{226}Ra did not contribute significantly to ^{222}Rn in lake water. Two sediment samples were collected from the WEDL for the calculation of the ^{222}Rn diffusion flux to the lake through a sediment equilibrium experiment. Table 1 shows the parameters of the sediment equilibrium experiment. Equation (8) was used to calculate the ^{222}Rn diffusion flux from sediment to lake water of 9.55 ± 2.00 Bq m^{-2} d^{-1} in the WEDL. Finally, the ^{222}Rn

https://doi.org/10.5194/hess-2021-364
Preprint. Discussion started: 7 September 2021

input flux of groundwater discharge was calculated to be 300.85 ± 168.55 Bq m^{-2} d^{-1}. The average ^{222}Rn concentration of the groundwater in the WEDL was 3242.54 ± 1281.61 Bq m^{-3}. Equation (3) was used to calculate the average LGD rate of 92.82 ± 51.98 mm d^{-1}. Remote sensing data were used to estimate the area of the WEDL during January 2020 of 173.22 km^2. By assuming that LGD occurred in all areas of the lake (Petermann et al., 2018; Liao et al., 2018), the flux of groundwater discharge to the WEDL could be calculated as 1.61 ± 0.90 $\times 10^7$ m^3 d^{-1}.

Table 1. The parameters of the sediment equilibrium experiment.

	A_0 (Bq m^{-3})	n	C_p (Bq m^{-3})	D_m(cm^2 s^{-1})	F_d	Area
Sed1	1112.5	0.421	18818.63	7.87×10^{-6}	8.13	WEDL
Sed2	1667.25	0.473	23037.53	7.87×10^{-6}	10.96	WEDL
Sed3	3112.5	0.512	39291.55	8.34×10^{-6}	20.56	EEDL

Different source and sink terms of the ^{222}Rn mass-balance model contribute to different proportions of total ^{222}Rn (Fig. 7a). ^{222}Rn originating from groundwater discharge to the lake dominated over other source terms, accounting for 96.93% of all ^{222}Rn input. The sediment diffusion ^{222}Rn flux was relatively small, accounting for only 3.07% of all ^{222}Rn input. Atmospheric loss constituted the largest sink of ^{222}Rn, accounting for 84.36% of all ^{222}Rn output. The decay of ^{222}Rn in lake water accounted for only 15.64% of all ^{222}Rn output.

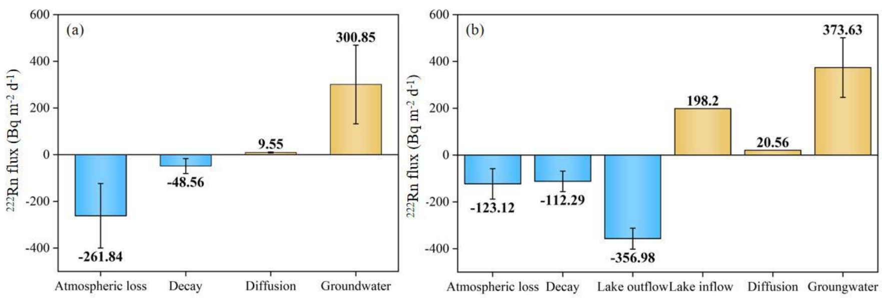

Figure 7. The proportions of different source and sink terms of ^{222}Rn in the Western part of East Dongting Lake (WEDL) **(a)** and East EDL (EEDL) **(b)**. The blue columns represent the sinks in the ^{222}Rn mass-balance model, expressed as a negative value; the orange columns represent the sources in the ^{222}Rn mass-balance model, expressed as a positive value.

4.2.2 Quantifying LGD in the EEDL

In the EEDL, input and output of water occurs from the upper reaches of the lake and from the northern part of the lake, respectively, with both these areas characterized by large discharge. Therefore,

Hydrology and Earth System Sciences Discussions

the ^{222}Rn input and output fluxes of surface water were considered in the ^{222}Rn mass-balance model even though the ^{222}Rn concentration of surface water was relatively low. The flow input to the EEDL was measured in the field whereas measures of flow output were obtained from the Hunan Provincial Hydrological Information Inquiry Network (http://skubaoxun.hnswkcj.com/wap/index_yq.asp).

Figure 7b shows the sink and source ^{222}Rn terms in the EEDL. The ^{222}Rn flux from lake water outflow was estimated to be 356.98 ± 44.82 Bq m^{-2} d^{-1}, accounting for 60.26% of all ^{222}Rn outputs. Equation (4) was used to calculate the atmospheric ^{222}Rn loss flux of 123.12 ± 65.04 Bq m^{-2} d^{-1}, accounting for 20.78% of all ^{222}Rn outputs. The average water depth in the EEDL during the study period was 3.9 m and the decay flux of ^{222}Rn was estimated to be 112.29 Bq m^{-2} d^{-1}, accounting for 18.96% of all ^{222}Rn outputs.

The sediment diffusion ^{222}Rn flux to the lake was calculated to be 20.56 Bq m^{-2} d^{-1}, accounting for only 3.47% of all ^{222}Rn inputs. The ^{222}Rn flux of inflow to the lake was 198.20 Bq m^{-2} d^{-1}, accounting for 33.46% of all ^{222}Rn inputs. Using the ^{222}Rn mass-balance model, the ^{222}Rn flux of groundwater discharge was estimated to be 373.63 ± 127.47 Bq m^{-2} d^{-1}, accounting for 63.07% of all ^{222}Rn inputs. The average ^{222}Rn concentration of groundwater in the EEDL was 9664.45 ± 6049.75 Bq m^{-3}. Equation (3) was used to calculate the groundwater discharge rate of 38.66 ± 21.07 mm d^{-1}. Remote sensing data indicated the area of the EEDL to be 88.62 km^2 in January, 2020. The flux of groundwater discharge to the EEDL was further calculated to be 3.43 ± 1.87 × 10^6 m^3 d^{-1}. The results showed that the LGD rate or flux to the WEDL was significantly higher than that of the EEDL.

4.3 Quantifying LGD-derived nutrient loads

Nutrients have a great influence on the ecological stability and water safety of lakes. Table S2, Table S3 and Fig. 8 show the concentrations of various nutrients in the lake water and groundwater of the WEDL and EEDL. The results clearly illustrate that the concentrations of various nutrients in groundwater generally exceeded those in lake water. Therefore, the discharge of groundwater to lake water posed a potential hazard to lake water quality.

https://doi.org/10.5194/hess-2021-364
Preprint. Discussion started: 7 September 2021

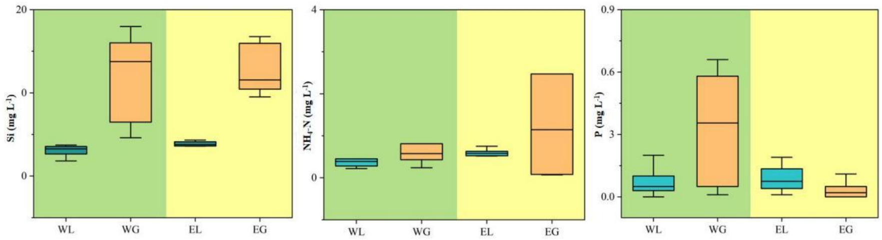

Figure 8. The concentrations of various nutrients in the lake water and groundwater of the Western part of East Dongting Lake (WEDL) and East EDL (EEDL). WL represents the lake water in WEDL; WG represents the groundwater in WEDL; EL represents the lake water in EEDL; EG represents the groundwater in EEDL.

The results of the ^{222}Rn mass-balance model showed that the LGD rates and fluxes in the WEDL and EEDL were 92.82 ± 51.98 mm d^{-1} and 38.66 ± 27.49 mm d^{-1}, respectively and 1.61 ± 0.90 $\times 10^7$ m^3 d^{-1} and 3.43 ± 2.44 $\times 10^6$ m^3 d^{-1}, respectively. The loads of nutrients contributed by LGD (g m^{-2} d^{-1}) was obtained by multiplying the LGD rate by the nutrients concentrations of groundwater and the LGD-derived nutrients fluxes (g d^{-1}) was obtained by multiplying the LGD loads by the lake area. The rank of nutrients originating from LGD according to input loads and fluxes to the WEDL was Si > NH_4-N > P (Table 2). The Si input load and flux associated with LGD were 1.12 g m^{-2} d^{-1} and 1.94×10^8 g d^{-1}, respectively, whereas that of NH_4-N was 0.24 g m^{-2} d^{-1} and 4.19×10^7 g d^{-1}, respectively, and that of P was 3.12×10^{-2} g m^{-2} d^{-1} and 5.40×10^6 g d^{-1}, respectively. The rank of nutrients originating from LGD according to input loads and fluxes to the EEDL was Si > NH_4-N > P (Table 2). The Si input load and flux associated with LGD was 0.49 g m^{-2} d^{-1} and 4.33×10^7 g d^{-1}, respectively, whereas that of NH_4-N was 8.22×10^{-2} g m^{-2} d^{-1} and 7.29×10^6 g d^{-1}, respectively, and that of P was 1.29×10^{-3} g m^{-2} d^{-1} and 1.14×10^5 g d^{-1}, respectively.

The input loads and fluxes of various nutrients originating from LGD to the WEDL far exceeded those to the EEDL (Fig. 9). The P load derived from LGD in the west exceeded that in the east by about a factor of 24. The input loads of Si and NH_4-N with LGD in the west exceeded those in the east by a factor of 2 to 3.

Table 2. The loads and fluxes of various nutrients originating from lacustrine groundwater discharge (LDG) within the East Dongting Lake, China.

Nutrients	Concentrations in groundwater (mg L^{-1})	Nutrients input loads originating from LGD (g m^{-2} d^{-1})	Nutrients input fluxes originating from LGD (g d^{-1})	Area
Si	12.10	1.12	1.94×10^8	WEDL
NH_4-N	2.61	0.24	4.91×10^7	

https://doi.org/10.5194/hess-2021-364
Preprint. Discussion started: 7 September 2021

P	0.34	3.12×10^{-2}	5.40×10^{6}	
Si	12.62	0.49	4.33×10^{7}	
NH_4-N	2.13	8.22×10^{-2}	7.29×10^{6}	EEDL
P	3.33×10^{-2}	1.29×10^{-3}	1.14×10^{5}	

Abbreviations: WEDL – western part of East Dongting Lake (WEDL); EEDL – Eastern part of EDL (EEDL).

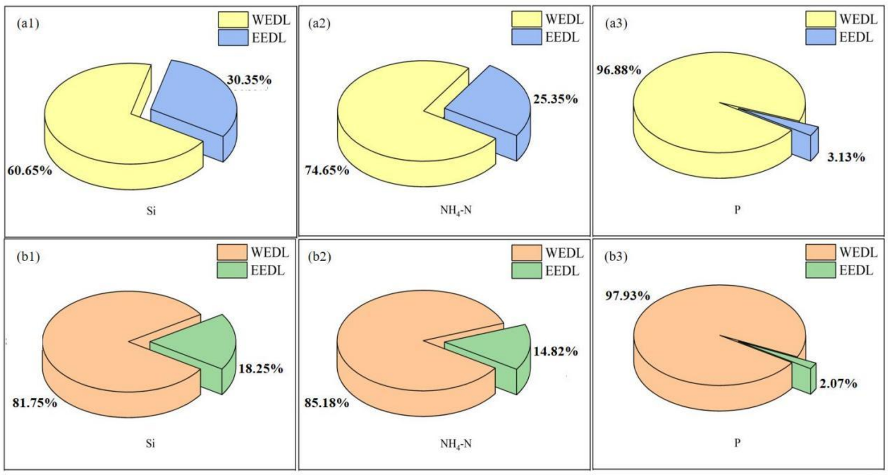

Figure 9. A comparison of nutrients input loads **(a)** and fluxes **(b)** originating from lacustrine groundwater discharge (LGD) between the western part of East Dongting Lake (WEDL) and the Eastern part of the EDL (EEDL), China.

4.4 Controls on contrasting spatial patterns of LGD and associated nutrient loads

The results from the ^{222}Rn mass-balance model indicated that the LGD rate in the WEDL was 2.4 times that in the EEDL, and the loads or fluxes of LGD-derived nutrients in the west generally exceeded that in the east by one order of magnitude. Given the contrasting geomorphy, surface hydrology, lakebed sediment lithology, hydrogeology and nutrient concentration levels of groundwater in the WEDL and EEDL, these factors may be inter-played and collaboratively lead to contrasting LGD rates and associated nutrient loads in two sides of EDL.

The EEDL is surrounded by hilly area, which limits the lateral extending of EEDL. As a result, the EEDL is characterized by relatively narrow and fast flowing. Owing to the intensive hydrodynamic process, more pebble, gravel and fine-coarse sand are transported and deposited in the lakebed. Under the long-term flushing imposed by artificial dredging, the EEDL is also characterized as deep flowing. Additionally, this steeper topography may result in a larger hydraulic gradient. Using the measurements of water level, the hydraulic gradient around the EEDL was estimated to be 0.004–0.006, significantly higher than that around the WEDL (0.0002–0.0015). These features appear to be more likely to produce a larger LGD rate. For example, in Lake Væng of Denmark, it was found that the high LGD was concentrated in the narrow littoral zones at the sandy lakebed, which was limited by a high terrace (Kazmierczak et al., 2021, 2020). In a small lake of Canada, Schmidt et al. (2010) found that higher LGD rates occurred in the sandy bottom of the lake that is not covered with organic material and limited by a bluff with steeper hydraulic gradients, compared to the lakebed consisting of silt with a high organic content covered by gyttja. However, contrary to our expectation, the low LGD rates were observed in the EEDL. In principle, the rate of LGD can be reflected by Darcy's law in which flow rate is determined by the hydraulic gradient between a lake and an aquifer and hydraulic conductivity, and the latter is determined by the permeability of the lakebed and the aquifer connected with the lake. Considering the large hydraulic gradient and high permeability of the lakebed in the EEDL, the low permeability of the connected aquifer should be a determining factor responsible for the low LGD rates in EEDL. Indeed, the lithology of the aquifer around the EEDL is mostly metamorphic and intrusive rock, which is characterized by a low specific yield of less than 5 m^3 h^{-1} m^{-1} (Zhao et al., 2020). Although larger water depth in the EEDL can lead to a better hydrologic connection with surrounding fissured aquifer that is deeply developed, quite low permeability of the aquifer still determines the low LGD rates. In addition, based on the results from water isotopes, the groundwater around the EEDL existed in a less confined environment, as a result of which frequent flushing can lead to low concentrations of nutrients. Coupled with low LGD rates, the LGD-derived nutrient loads will be proportionally lower.

On the contrast, the WEDL area is mainly surrounded by alluvial-lacustrine plains. The low-lying and flat topography in this area can lead to a weak hydrodynamic environment, which can further make more clay, silty clay and fine-grained sand deposited in the lakebed (HGSI, 2016). Under the long-term silting, the WEDL is characterized by relatively shallow water depth. These super-surface features coupled with quite low hydraulic gradients make it seem impossible to have high LGD rates in this area. Therefore, the high LGD rates should be controlled by underground geological structures. The main aquifers around the WEDL are the phreatic aquifer and porous confined aquifer. The phreatic aquifer is weakly permeable with a specific yield still less than 5 m^3 h^{-1} m^{-1} and an uneven thickness of 5–20 m (HGSI, 2016). The phreatic aquifer is connected with the shallow area of the lake. The porous confined aquifer is situated below the weakly permeable layer and is mainly composed of fine-medium sand with a large thickness of 50–150 m. This aquifer is more likely to be connected with the deeper area of the lake. This aquifer has a higher specific yield of 5–10 m^3 h^{-1} m^{-1} (HGSI, 2016). Despite somewhat higher specific yield, one order of magnitude lower hydraulic gradients still makes it seem impossible to have high LGD rates in the WEDL. Therefore, the permeability of the porous aquifer is probably enlarged by some preferential pathways, which further leads to high LGD rates in the WEDL.

On a macro scale, a buried paleo-channel, i.e., the ancient channel of the Yuanjiang River, composed of coarse sand and gravel (Xu et al., 2019; Liang et al., 2001), was detected in the second aquifer within the WEDL area (Fig. S1). This buried paleo-channel was formed due to the filling of incised valley formed during the Last Glacial Maximum, and extended to the west shore of the WEDL (Xu et al., 2019). Therefore, this paleo-channel probably acts as a preferential pathway of groundwater discharge to the lake. Alternatively, on a smaller scale, it has been widely the permeability of the lakebed is not only determined by grain size, but also by the roots of vegetation (Yang et al., 2019; Richards and Reddy, 2007). Despite finer sediment size, the shallow area of the WEDL hosts a large number of plants, including reed, Carex cinerascens and Phalaris arundinacea (Zhang et al., 2020; Yang et al., 2019). The roots of these plants can produce various cracks, thereby increasing the permeability of the lakebed (Smart et al., 2013). Therefore, the small channels produced by the roots of plants could be another preferential pathway facilitating high LGD rates in the WEDL. The special geological conditions in the WEDL area could be also internally associated with high nutrient concentrations in groundwater. This is because ammonium and phosphorus in groundwater around the WEDL have been found to be geogenic, and their accumulation is closely associated with abundant buried organic matter (Huang et al., 2021). This abundant organic matter pool is probably closely associated with rapid burial of sediments in incised valley during the Last Deglaciation and continuous deposition with lakes during the Holocene (Polizzotto et al., 2008; Wang et al., 2019). Coupled with higher concentrations of these nutrients in groundwater, the high LGD rates in the WEDL produce the LGD-derived nutrient loads exceeding that in the east by one order of magnitude (Fig. 10).

In practice, the WEDL faces a high risk of eutrophication and is therefore the most susceptible part of the lake to eutrophication (Qing et al., 2020; Xue et al., 2020; Huang et al., 2015). Most previous studies concluded that the WEDL is relatively independent from the rest of the lake and that water in the WEDL has a long residence time, with both these factors contributing to a high risk of eutrophication (Chen et al., 2021; Lin et al., 2018). LGD-derived nutrients in the WEDL may also

https://doi.org/10.5194/hess-2021-364
Preprint. Discussion started: 7 September 2021

contribute to a greater risk of eutrophication, although this factor has not previously been considered. Therefore, the role of groundwater in securing water and ecological resources in the WEDL may be important. The results of the present study highlight the need for integrating groundwater and lake water within the management of the Dongting Lake, with a focus on the WEDL.

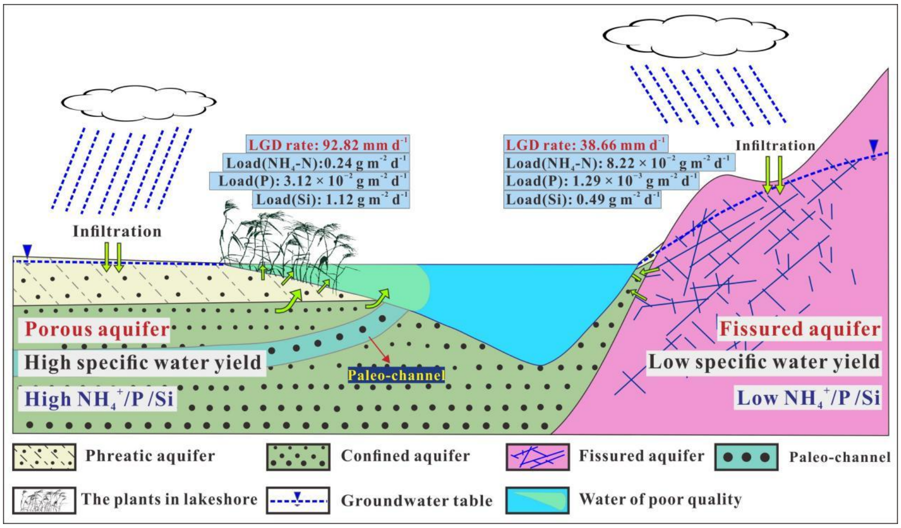

Figure 10. A conceptual model for the contrasting spatial patterns of groundwater discharge and associated nutrients input in the East Dongting Lake, central China. WEDL and EEDL represents West EDL and East EDL, respectively. The higher LGD rate and loads of LGD-derived nutrients were detected in the porous aquifer-lake system compared with the fissured aquifer-lake system.

5 Conclusion

This study used radon mass-balance model together with water chemistry and existing geological data to identify and quantify the spatial differences of LGD and associated nutrients input in two sides with contrasting geological conditions of East Dongting Lake within central Yangtze catchment and discuss the influence of geology on the spatial differences. It was found that LGD rates were 38.66 ± 21.07 mm d^{-1} in the east EDL which is characterized by hilly geomorphy, deep/fast/narrow flowing, coarse-grained lakebed and large hydraulic gradients (0.004–0.006). The west EDL is characterized by alluvial-lacustrine plain geomorphology, shallow/sluggish flowing, clayey or silty lakebed and low hydraulic gradients (0.0002–0.0015), which makes it seem impossible to have high LGD rates in the west EDL. However, the LGD rates were determined to be remarkably higher in the west EDL (92.82 ± 51.98 mm d^{-1}). The remaining factor responsible for the higher LGD rates in the west EDL is the permeability of the porous aquifer connected with the lake, which is enlarged by some preferential pathways including large-scale buried paleo-channel and small-scale plant roots.

The geological conditions were further inter-played with hydrogeological environment and groundwater quality. The groundwater around the east EDL existed in a less confined environment, and frequent flushing led to low concentrations of nutrients. On the contrast, rapid burial of sediments during the Last Deglaciation and deposition of paleo-lake sediments during the Holocene formed an organic-rich and reducing environment, which facilitated the enrichment of geogenic nutrients. As a result, the loads of LGD-derived nutrients in the west were determined to generally exceed that in the east by one order of magnitude. In practice, future water resource management and ecological protection of Dongting Lake should focus on groundwater discharge in west EDL.

Data availability. The topographical information is from Geospatial data cloud (http://www.gscloud.cn/sources/index?pid=302). Other data is in the attached file. Address inquiries to the corresponding author.

Author contributions. This research was conceived by YD and XS. YD contributed ideas for analyses. YD, XS and HF carried out the field work. XS analyzed the data, and wrote the paper with input from all the authors. TM supervised and provided project support.

Competing interests. The authors declare that they have no conflict of interest.

Acknowledgments. The research was funded by National Natural Science Foundation of China (No. 41521001, No. 41977174, No. 41907173, and No. 4201001051), Project of Hubei Provincial Key Research and Development (No. 2020BCA088), Project of China Geological Survey (No. DD20190263).

Reference

Birks, S.J., Jeffries, D., and Yi, Y.: Regional trends in evaporation loss and water yield based on stable isotope mass balance of lakes: the Ontario Precambrian shield surveys, J. Hydrol., 544, 500-510, https://doi.org/10.1016/j.jhydrol.2016.11.016, 2017.

Blume, T., Krause, S., Meinikmann, K., and Lewandowski, J.: Upscaling lacustrine groundwater discharge rates by fiber-optic distributed temperature sensing, Water Resour. Res., 49, 7929-7944, https://doi.org/10.1002/2012WR013215, 2013.

Born, S.M., Smith, S.A., and Stephenson, D.A.: Hydrogeology of glacial-terrain lakes, with management and

https://doi.org/10.5194/hess-2021-364
Preprint. Discussion started: 7 September 2021

planning applications, J. Hydrol., 43, 7-43, https://doi.org/10.1016/0022-1694(79)90163-X, 1979.

Boudreau, B.P.: The diffusive tortuosity of fine-grained unlithified sediments, Geochim. Cosmochim. Acta., 60(16), 3139-3142, https://doi.org/10.1016/0016-7037(96)00158-5, 1996.

Burnett, W.C., Wattayakorn, G., Supcharoen, R., Sioudom, K., Kum, V., Chanyotha, S., and Kritsananuwat, R.: Groundwater discharge and phosphorus dynamics in a flood-pulse system: tonle sap lake, cambodia, J. Hydrol., 549, 79-91, https://doi.org/10.1016/j.jhydrol.2017.03.049, 2017.

Chen, X., Ou, M.W., Jia, S., and Li, Y.: Remote Sensing Retrieval and Evaluation of Chlorophyll-a Concentration in East Dongting Lake, China. IOP Conference Series, Environ Earth Sci, 668(1), https://doi.org/10.1088/1755-1315/668/1/012035, 2021.

Cheng, K., Luo, X, and Jiao, J.J.: Two-decade variations of fresh submarine groundwater discharge to tolo harbour and their ecological significance by coupled remote sensing and radon-222 model, Water Res., 178, 115866, https://doi.org/10.1016/j.watres.2020.115866, 2020.

Corbett, D.R., Burnett, W.C., Cable, P.H., and Clark, S.B.: Radon tracing of groundwater input into Par Pond, Savannah River Site, J. Hydrol., 203, 209-227, https://doi.org/10.1016/S0022-1694(97)00103-0, 1997.

Corbett, D.R., Burnett, W.C., Cable, P.H., and Clark, S.B.: A multiple approach to the determination of radon fluxes from sediments, Radioanal Nucl Chem, 236(1-2), 247-253, https://doi.org/10.1007/BF02386351, 1998.

Dabrowski, J.S., Charette, M.A., Mann, P.J., Ludwig, S.M., and Henderson, P.B.: Using radon to quantify groundwater discharge and methane fluxes to a shallow, tundra lake on the yukon-kuskokwim delta, alaska, Biogeochemistry, 148(1), 69-89, https://doi.org/10.1007/s10533-020-00647-w, 2020.

Dimova, N., Paytan, A., Kessler, J.D., Sparrow, K., Garcia-Tigreros K.F., Lecher, A.L., Murray, J., and Tulaczyk, S.M.: The current magnitude and mechanisms of groundwater discharge in the Arctic: a case study from Alaska, Environ. Sci. Technol., 49(20), 12036-12043, https://doi.org/10.1021/acs.est.5b02215, 2015.

Dimova, N.T., Burnett, W.C., Chanton, J.P., and Corbett, J.E.: Application of radon-222 to investigate groundwater discharge into small shallow lakes. J. Hydrol., 486, 112–122. https://doi.org/10.1016/j.jhydrol.2013.01.043. 2013.

Dimova, N.T. and Burnett, and W.C.: Evaluation of groundwater discharge into small lakes based on the temporal distribution of radon-222, Limnol. Oceanogr., 56, 486-494, https://doi.org/10.4319/lo.2011.56.2.0486, 2011.

Gilfedder, B.S., Frei, S., and Hofmann, H., Cartwright, I.: Groundwater discharge to wetlands driven by storm and flood events: Quantification using continuous Radon-222 and electrical conductivity measurements and dynamic mass-balance modelling, Geochim. Cosmochim. Acta., 165, 161–177, https://doi.org/10.1016/j.gca.2015.05.037, 2015.

Hare, D.K., Boutt, D.F., Clement, W.P., Hatch, C.E., Davenport, G., and Hackman, A.: Hydrogeological controls on spatial patterns of groundwater discharge in peatlands, Hydrol. Earth Syst. Sci., 21, 6031-6048, https://doi.org/10.5194/hess-21-6031-2017, 2017.

https://doi.org/10.5194/hess-2021-364
Preprint. Discussion started: 7 September 2021

Hydrology and Earth System Sciences Discussions
Open Access

Hu, C., Fang, C., and Cao, W.: Shrinking of Dongting Lake and its weakening connection with the Yangtze River: analysis of the impact on flooding, International Journal of Sediment Research, 30(3), 256-262, https://doi.org/10.1016/j.ijsrc.2014.05.001, 2015.

Hu, W.M., Li, G., Gao, Z.h., Jia, G.Y., Wang, Z.C., and Li, Y.: Assessment of the impact of the Poplar Ecological Retreat Project on water conservation in the Dongting Lake wetland region using the InVEST model, Sci. Total Environ., 733, https://doi.org/10.1016/j.scitotenv.2020.139423, 2020.

Huang Y.F., Wang, J.S., and Yang, M.: Dynamic Pollutant Absorption Capacity of East Dongting Lake Based on relationship among Water Level, Area and Volume, Journal of Yangtze River Scientific Research Institute, 35(09),12-16, https://doi.org/10.11988/ckyyb.20180533, 2018 (in Chinese).

Huang, B., Jiang, H., Qian, Z., and Long, Q.B.: Spatial Distribution Characteristics of Groundwater Quality in the Dongting Lake Area Based on ArcGIS, China Rural Water and Hydropower, (10), 34-37, doi:CNKI:SUN:ZNSD.0.2019-10-007, 2019 (in chinese).

Huang, J., Wang, X.X., Xi, B.D., Xu, QJ., Tang, Y., Jia, K.L., Huo, S.L., Da, A., Gao, R.Z., Liu, H.L., Li, X.G., Liu, M.M., and Mao, J.Y.: Long-term variations of TN and TP in four lakes fed by Yangtze River at various timescales, Springer Berlin Heidelberg, 74(5), https://doi.org/10.1007/s12665-015-4714-y, 2015.

Huang, Y.M., 2013. Study of variable characteristics of Stable Water Isotope Composition in Water Cycle and Its Influnce Mechanism in the Dongting Lake Basin, Hunan Normal University (in Chinese).

Huang, Y.W, Du, Y., Ma, T., Deng, Y.M., and Leng, Z.C.: Dissolved organic matter characterization in high and low ammonium groundwater of Dongting plain, central china, Ecotoxicol. Environ. Saf., 208, 111779, https://doi.org/10.1016/j.ecoenv.2020.111779, 2021.

Hunan Geological Survey Institute.: Investigation and Evaluation of Groundwater Resources and Environmental Problems in Jianghan-Dongting Plain (Hunan) Report, 2016.

Kazmierczak, J., Postma, D., Muller, S., Jessen, S., Nilsson, B., Czekaj, J., and Engesgaard, P.: Groundwater-controlled phosphorus release and transport from sandy aquifer into lake, Limnol. Oceanogr., https://doi.org/10.1002/lno.11447, 2020.

Kidmose, J., Nilsson, B., Engesgaard, P., Frandsen, M., Karan, S., Landkildehus, F., Søndergaard, M., and Jeppesen, E.: Focused groundwater discharge of phosphorus to a eutrophic seepage lake (Lake Væng, Denmark): implications for lake ecological state and restoration, Hydrogeol. J., 21, 1787-1802, https://link.springer.com/article/10.1007/s10040-013-1043-7, 2013.

Kluge, T., Ilmberger, J., von Rohden, C., and Aeschbach-Hertig, W.: Tracing and quantifying groundwater inflow into lakes using a simple method for radon-222 analysis, Hydrol. Earth Syst. Sci., 11, 1621-1631, https://doi.org/10.5194/hess-11-1621-2007, 2007.

Kong, F.C, Sha, Z.J, Luo, X., Du, J.Z, Jiao, J.J., Moore, W.S., Yang, Y.K, and Su, W.G.: Evaluation of lacustrine groundwater discharge and associated nutrients, trace elements and DIC loadings into Qinghai Lake in

https://doi.org/10.5194/hess-2021-364
Preprint. Discussion started: 7 September 2021

Qinghai-Tibetan Plateau, using radium isotopes and hydrological methods, Chem. Geol., 510, 31-46, https://doi.org/10.1016/j.chemgeo.2019.01.020, 2019.

Lewandowski, J., Meinikmann, K., Nützmann, G., and Rosenberry, D.O.: Groundwater-the disregarded component in lake water and nutrient budgets. Part 2: effects of groundwater on nutrients, Hydrol. Process., 29, 2922-2955. https://doi.org/10.1002/hyp.10384, 2015.

Lewandowski, J., Meinikmann, K., Ruhtz, T., Pöschke, F., and Kirillin, G.: Localization of lacustrine groundwater discharge (LGD) by airborne measurement of thermal infrared radiation, Remote Sens Environ., 138:119-125, https://doi.org/10.1016/j.rse.2013.07.005, 2013.

Li, Y., and Yang, W.Y.: The Evolutionary Trend of the Runoff and the Water Challenge Faced by Agriculture in the Three Outlets Area of Dongting Lake, China Rural Water and Hydropower, (11), 86-92+100, https://doi.org/10.3969/j.issn.1007-2284.2016.11.021, 2016 (in Chinese).

Liang, X., Zhang, R.Q., Pi, J.G., Zhang, G.L., and Sun, X.L.: Characteristics of Tectonic Movement of Dongting Basin in the Quaternary Period, Bulletin of Geological Science and Technology, 20(002), 11-14, https://doi.org/10.3969/j.issn.1000-7849, 2001 (in Chinese).

Liao, F. , Wang, G.C , Yi, L.X., Shi, Z.M., Cheng, G.Q., Kong, Q.M., Mu, W.Q., Guo, Liang., Cheng, K., Dong, Na., and Liu, C.L.: Identifying locations and sources of groundwater discharge into poyang lake (eastern china) using radium and stable isotopes (deuterium and oxygen-18), Sci. Total Environ., 740, 140163, https://doi.org/10.1016/j.scitotenv.2020.140163, 2020.

Liao, F., Wang, G.C., Shi, Z.M., Cheng, G.Q., Kong, Q.M., Mu, W.Q., and Guo, L.: Estimation of groundwater discharge and associated chemical fluxes into Poyang Lake, China: approaches using stable isotopes (δD and $\delta^{18}O$) and radon, Hydrogeol. J., 26 (5), 1625-1638, https://doi.org/10.1007/s10040-018-1793-3, 2018.

Lin, J., Lyu, H., Miao, S., Pan, Y., Wu, Z.M., Li,Y.M., and Wang, Q.: A two-step approach to mapping particulate organic carbon (POC) in inland water using OLCI images, Ecol. Indic., 90, 502-512, https://doi.org/10.1016/j.ecolind.2018.03.044, 2018.

Liu, X.Q., Yi, F.H., Luan, Z.Y., and Wang, D.N.: Processes of East Dongting Lake in recent period, Journal of Sediment Research, (4), 25-32, https://doi.org/10.16239/j.cnki.0468-155x.2019.04.005, 2019 (in chinese).

Long, Y.N., Yan S.X., Jiang C.B., Wu C.S., Li Z.W., and Tang R.: A new method for extracting lake bathymetry using multi-temporal and multi-source remote sensing imagery: A case study of Dongting Lake, Acta Geographica Sinica, 74(07), 1467-1481, https://doi.org/10.11821/dlxb201907015, 2019 (in Chinese).

Luo, X., Kuang, X.X., Jiao, J.J., Liang, S.H., Mao, R., Zhang, X.L., and Li, H,: Evaluation of lacustrine groundwater discharge, hydrologic partitioning, and nutrient budgets in a proglacial lake in the Qinghai-Tibet Plateau: using ^{222}Rn and stable isotopes, Hydrol. Earth Syst. Sci., 22, 5579-5598, https://doi.org/10.5194/hess-22-5579-2018, 2018.

Luo, X., and Jiao, J.J.: Submarine groundwater discharge and nutrient loadings in Tolo Harbor, Hong Kong using

https://doi.org/10.5194/hess-2021-364
Preprint. Discussion started: 7 September 2021

Hydrology and Earth System Sciences
Discussions

multiple geotracer-based models, and their implications of red tide outbreaks, Water Resour. Res., 102, 11-31, 2016.

Luo, X., Jiao, J.J., Moore, W., and Lee, C.M.: Submarine groundwater discharge estimation in an urbanized embayment in Hong Kong via short-lived radium isotopes and its implication of nutrient loadings and primary production, Mar Pollut Bull., 82(1-2), 144-154, https://doi.org/10.1016/j.marpolbul.2014.03.005, 2014.

MacIntyre, S., Wanninkhof, R., and Chanton, J.: Trace gas exchange across the air-water interface in freshwater and coastal marine environments, Wiley-Blackwell., 1995.

Meinikmann, K., Lewandowski, J., and Nützmann, G.: Lacustrine groundwater discharge: combined determination of volumes and spatial patterns, J. Hydrol., 502, 202-211, https://doi.org/10.1016/j.jhydrol.2013.08.021, 2013.

Pan, T., Wu, S.H., Dai, E.F., Liu, and Y.J.: Spatiotemporal variation of water source supply service in three rivers source area of China based on InVEST model, Chinese Journal of Applied Ecology, 24(1), 183-189, 2013.

Peterson, R.N., and Santos, I.R.,Spatiotemporal variation of water source supply service in three rivers source area of China based on InVEST model Burnett, W.C.: Evaluating groundwater discharge to tidal rivers based on a Rn-222 time-series approach, Estuarine Coastal and Shelf Science, 86(2), 165-178, https://doi.org/10.1016/j.ecss.2009.10.022, 2010.

Petermann, E., Gibson, J.J., Knoeller, K., Pannier, T., Weiss, H., and Schubert, M.: Determination of groundwater discharge rates and water residence time of groundwater-fed lakes by stable isotopes of water (^{18}O, ^{2}H) and radon (^{222}Rn) mass balances, Hydrol. Process., 32(6), 805-816, https://doi.org/10.1002/hyp.11456, 2018.

Polizzotto, M.L., Kocar, B.D., Benner, S.G., Sampson, M., and Fendorf, S.: Near-surface wetland sediments as a source of arsenic release to ground water in Asia, Science, 454, 505-508, https://doi.org/10.1038/nature07093, 2008.

Qin, W.J., Han D.M., Song, X.F., and Liu, S.H.: Environmental isotopes (δ^{18}O, δ^{2}H, ^{222}Rn) and hydrochemical evidence for understanding rainfall-surface water-groundwater transformations in a polluted karst area-sciencedirect, J. Hydrol., 592, https://doi.org/10.1016/j.jhydrol.2020.125748, 2020.

Rosenberry, D.O., Lewandowski, J., Meinikmann, K., and Nützmann, G.: Groundwater-the disregarded component in lake water and nutrient budgets. Part 1: effects of groundwater on hydrology, Hydrol. Process., 29, 2895-2921, https://doi.org/10.1002/hyp.104032015.

Roy, J.W., and Hayashi, M.: Groundwater exchange with two small alpine lakes in the Canadian Rockies, Hydrol. Process., 22, 2838-2846, https://doi.org/10.1002/hyp.6995, 2008.

Schmidt, A., Gibson, J.J., Santos, I.R., Schubert, M., Tattrie, K., and Weiss, H.: The contribution of groundwater discharge to the overall water budget of two typical Boreal lakes in Alberta/Canada estimated from a radon mass balance, Hydrol. Earth Syst. Sci., 14, 79-89, https://doi.org/10.5194/hess-14-79-2010, 2010.

Schmidt, A., Stringer, C.E., Haferkorn, U., and Schubert, M.: Quantification of groundwater discharge into lakes using radon-222 as naturally occurring tracer, Environ. Geol., 56(5), 855-863, https://doi.org/10.1007/s00254-008-1186-3, 2009.

Schneider, R.L., Negley, T.L., and Wafer, C.: Factors influencing groundwater seepage in a large, mesotrophic lake in New York, J. Hydrol., 310, 1-16, https://doi.org/10.1016/j.jhydrol.2004.09.020, 2005.

Schubert, M., Scholten, J., Schmidt, A.,Comanducci, J.F, Pham, M., Mallast, U., and Knoellerl, K.: Submarine groundwater discharge at a single spot location: evaluation of different detection approaches, Water, 6(3), 584-601, https://doi.org/10.3390/w6030584, 2014.

Smart, R.P., Holden, J., Dinsmore, K.J., Baird, A.J., Billett, M.F., Chapman, P.J., and Grayson, R.: The dynamics of natural pipe hydrological behaviour in blanket peat, Hydrol. Process., 27, 1523-1534, https://doi.org/10.1002/hyp.9242, 2013.

Stets, E.G., Winter, T.C., Rosenberry, D.O., and Striegl, R.G.: Quantification of surface water and groundwater flows to open and closedbasin lakes in a headwaters watershed using a descriptive oxygen stable isotope model, Water Resour. Res., 46, W03515, https://doi.org/10.1029/2009WR007793, 2010.

Sun, S.R., Xie P., Zhao, J.Y., Sang, Y.F., Ning, M.J., and Zhou, H.: Variability in the annual flood peak discharge and water level in three outlets of Lake Dongting, Journal of Lake Sciences, 30(03), 812-824, https://doi.org/10.18307/2018.0323, 2018 (in Chinese).

Sun, X.L., Du, Y., Deng, Y.M., Fan, H.C., Tao, Y.Q., and Ma, T.: Contribution of groundwater discharge and associated contaminants input to dongting lake, central china, using multiple tracers (^{222}Rn, ^{18}O, Cl^-), Environ Geochem Hlth, 43, 1239-1255, https://doi.org/10.1007/s10653-020-00687-z, 2020.

Sun, X.L., Du, Y., Deng, Y.M., and Tao, Y.C.: Contribution and its temporal variation of groundwater discharge to the water mass balance of Dongting Lake from 1996 to 2017, Earth Science, 1-18, https://doi.org/10.3799/dqkx.2020.195, 2020 (in chinese).

Tecklenburg, C., and Blume, T.: Identifying, characterizing and predicting spatial patterns of lacustrine groundwater discharge, Hydrol. Earth Syst. Sci., 21, 5043-5063, https://doi.org/10.5194/hess-21-5043-2017, 2017.

Wallace, H., Wexler, E.J.. Malott, S., and Robinson, C.E.: Evaluating lacustrine groundwater discharge to a large glacial lake using regional scale radon-222 surveys and groundwater modelling, Hydrol. Process, 35(4), https://doi.org/10.1002/hyp.14165, 2021.

Wallace, H., Tao, J., and Robinson, C.E.: Hydrogeological controls on heterogeneous groundwater discharge to a large glacial lake, Journal of Great Lakes Research, 46(3), 476-485, https://doi.org/10.1016/j.jglr.2020.03.006, 2020.

Wang, Q., Ou, F.P., Zang, L., and Lu, S.Y.: Changes of Water Environment in Dongting Lake and its Impact Analysis after the Three Gorges project operation, Journal of Yangtze River Scientific Research Institute, 24(11), 1843-1849, doi:CNKI:SUN:CJLY.0.2015-11-006, 2015a. (in Chinese)

https://doi.org/10.5194/hess-2021-364
Preprint. Discussion started: 7 September 2021

Wang, S.R., Meng, W., Jin, X.C., Zheng, B.H., Zhang, L., and Xi, H.Y.: Ecological security problems of the major key lakes in china, Environmental Earth Sciences, 74(5), 3825-3837, https://doi.org/10.1007/s12665-015-4191-3, 2015b.

Wang, Y.X., Pi, K.F., Fendorf, S., Deng, Y.M., and Xie, X.J.: Sedimentogenesis and hydrobiogeochemistry of high arsenic Late Pleistocene-Holocene aquifer systems, Earth-Science Reviews, 189, 79-98, https://doi.org/10.1016/j.earscirev.2017.10.007, 2019.

Wu, H.W., Zhang, X.P., Sun, G.L., Hunag, Y.M., Shen, L., and Guo, L.X.: Variations of Stable Isotopic Characteristics of Atmospheric Precipitation from Changsha, Hunan, Resources and Environment in the Yangtze Basin, 21(5) :540-546, doi:CNKI:SUN:CJLY.0.2012-05-005, 2012 (in Chinese).

Xie, P.: Ecological Impacts of Three Gorges Dam on lakes Dongting and Poyang, Resources and Environment in the Yangtze Basin, 26(10), 1607-1618, 2017 (in Chinese).

Xiong, J., Yu, F.Q., Tian, Q., Huang D.Z., and Li, L.Q.: The evolution of water quality and nutrient condition in Lake Dongting in recent 30 years, Journal of Lake Sciences, 28(06), 1217-1225, https://doi.org/10.18307/2016.0607, 2016 (in Chinese).

Xu, Y., Lai, Z., and Li, C.: Sea-level change as the driver for lake formation in the yangtze plain-a review, Glob Planet Change, 181, 102980, https://doi.org/10.1016/j.gloplacha.2019.102980, 2019.

Xue, K., Ma, R.H., Shen, M., Li, Y., Duan, H.T., Cao, Z.G., Wang, D., and Xiong, J.F.: Variations of suspended particulate concentration and composition in Chinese lakes observed from Sentinel-3A OLCI images, Sci. Total Environ., 721, https://doi.org/10.1016/j.scitotenv.2020.137774, 2020.

Xue, Y., Liu, F., Liu, J, and Sun, Y.: Annual variation characteristics of eutrophication in dongting lake, china, Water Management, 173(4), 1-18, https://doi.org/10.1680/jwama.19.00026, 2020.

Yang, J., Yu, Z., Yi, P., Frape, S.K., Gong, M., and Zhang, Y.: Evaluation of surface water and groundwater interactions in the upstream of Kui river and Yunlong lake, Xuzhou, China, J. Hydrol., 583, 124549, https://doi.org/10.1016/j.jhydrol.2020.124549, 2020.

Yang, N., Li, J.H., Mo, W.B., Luo, W.J., Wu, D., Gao, W.C., and Sun, C.H.: Water depth retrieval models of East Dongting Lake, China, using GF-1 multi-spectral remote sensing images, Glob Ecol Conserv, 22, https://doi.org/10.1016/j.gecco.2020.e01004, 2020.

Yang, N., Mo, W.B., Zhang, X., Luo, W.J., Zhang, C.M., Zhao, Y.L., and Ma, F.F.: Yang Analysis of vegetation spatio-temporal variation based on NDVI of east Dongting wetland over the past 30 years, Journal of Central South University of Forestry and Technology, 039(007), 19-30, https://doi.org/10.14067/j.cnki.1673-923x.2019.07.003, 2019 (in Chinese).

Yi, L.: The Evolution of River-lake Relationship's in the Middle Region of Yangtze River During Historical Period: Take Dongting Lake and Poyang Lake as Examples, Wuhan University, 2017 (in Chinese).

Yi, P., Luo, H., Chen, L., Yu, Z.B., Jin, H.J., Chen, X.B., Wan, C.W., Aldahan, A., Zheng, M.J., and Hu, Q.F.:

Evaluation of groundwater discharge into surface water by using radon-222 in the source area of the yellow river, qinghai-tibet plateau, Journal of Environmental Radioactivity, 192, 257, https://doi.org/10.1016/j.jenvrad.2018.07.003, 2018.

Yu, S.C.,Wang, L.C., Xia, W.P., Yu, D.Q., Li, C.A., and He, Q.H.: Spatio-temporal evolution of riparian lakes in Dongting Lake area since the late Qing Dynasty, Acta Geographica Sinica, 75(11), 2346-2361, 2020 (in chinese).

Zhan, L.C., Chen, J.S., and Zhang, S.Y.: Characteristics of stable isotopes in precipitation, surface water and groundwater in the Dongting Lake region. Advances in Water Science, 25(03), 327-335, 10.14042/j.cnki.32.1309.2014.03.003, 2014 (in chinese).

Zhang, Q., Zhou, M., Li Q.L., Sun, L., Hu M.H., and Qiu, S.: GF5-Based Water Quality Monitoring of East Dongting Lake, China, IOP Conference Series: Earth and Environmental Science, 509(1), 10.1088/1755-1315/509/1/012031, 2020.

Zhang, Y.H., Lai, X.J., Zhang, L., Song, K.S., Yao, X., Gu, L.H., and Pang, C.C.: The influence of aquatic vegetation on flow structure and sediment deposition: a field study in dongting lake, china. J. Hydrol., 584, 124644, https://doi.org/10.1016/j.jhydrol.2020.124644, 2020.

Zhao, D., Wang, G.C, Liao, F., Yang, N.A, Jiang, W.J, Guo, L., Liu, C.L, and Shi, Z.M.: Groundwatersurface water interactions derived by hydrochemical and isotopic (^{222}Rn, deuterium, oxygen-18) tracers in the Nomhon area, Qaidam Basin, NW China, J. Hydrol., 565, 650-661, https://doi.org/10.1016/j.jhydrol.2018.08.066, 2018.

Zhao, X.Y.Z., Yu, W., Xiao, P., Guan, Y.T., and Yao, T.F.: Discussion on Compilation Thought and Moth-odology of 1:450000 Hydrogeological Map of the Jianghan-Dongting Plain, South China Geology, 36(4), 396-403, 2020 (in Chinese).

Zheng, H., Li, Y., Robinson, B.E., Liu, G., Ma, D., Wang, F., Lu, F.: Ouyang, Z., and Daily, G.C.: Using ecosystem service trade-offs to inform water conservation policies and management practices, Frontiers in ecology and the environment, 14, 527-532, https://doi.org/10.1002/fee.1432, 2016.

Zou, Y.A., Zhang, P.Y., Zhang, S.Q., Chen X.S., Li F., Deng Z.M., Yang, S., Zhang H., Li, F.Y., and Xie, Y.H.: Crucial sites and environmental variables for wintering migratory waterbird population distributions in the natural wetlands in East Dongting Lake, China, Sci. Total Environ., 655, 147-157, https://doi.org/10.1016/j.scitotenv.2018.11.185, 2019.